63. Temporal modelling of grape phenology using a monitoring camera sensor

F. Rançon[1,2,*], B. Keresztes[1,2], V.H.H. Pham[1], A. Deshayes[1], M. Mabrouk[1], J.P. Da Costa[1,2] and C. Germain[1,2]

[1] *Université Bordeaux, CNRS, Bordeaux INP, IMS, UMR 5218, F-33400 Talence, France*

[2] *Bordeaux Sciences Agro, F-33170 Gradignan, France; florian.rancon@agro-bordeaux.fr*

Abstract

In this study, a daily grape images dataset derived from a set of 7 monitoring cameras (Vinelapse, IMS Laboratory) is presented. Features describing the joint evolution of grape colour, texture and berry sizes were then extracted using image processing. The relevance of a flexible statistical framework (generalized additive model) to model non-linear trends and identify periods of change in the time series is presented. Results show steady changes can be identified at certain periods, while accounting for model uncertainty. This illustrates the potential of daily grape images time series to compare the phenological behaviour of plants within the same vineyard.

Keywords: generalized additive models, grapevine phenology, image processing, time series

Introduction

Grapevine phenology describes recurring growth cycles, such as the reproductive cycle ranging from budburst to harvest. From an operational point of view, phenological knowledge can be used for targeted site-specific management (e.g. fungicide application, irrigation strategies, harvest planning). Indeed, phenology is well known for its spatial variability, since overall plant development is the result of many combined phenomena at different spatial scales (Verdugo-Vásquez *et al.*, 2016), including climatic variables (García de Cortázar-Atauri *et al.*, 2017). However, directly measuring phenological variables of interest is often difficult and time consuming. Precision viticulture combines innovative sensing technologies with variable rate technologies (VRT) on agricultural machinery to tackle these issues (Ammoniaci *et al.*, 2021).

This paper focuses on the potential uses of optical sensors to extract grape phenology information. The main appeal of imaging sensors lies in the flexibility they offer, proving useful for various tasks such as vigour estimation or disease detection (Tardif *et al.*, 2022) at affordable costs. Their major drawback, however, is the challenge to extract relevant information from the images in a consistent way. In that regard, autonomous camera sensors are a promising way to sample continuous temporal information on selected parts of the vineyard. Prior to this study, a few autonomous imaging sensors have been developed for viticulture (Mendes *et al.*, 2022) or more generally for outdoor biodiversity monitoring (Darras *et al.*, 2024). Vinelapse is a camera sensor developed by the IMS laboratory, whose main asset is the inclusion of controlled lighting, meaning vine images taken at different dates can be directly compared. Still, the processing and statistical analysis of image datasets generated by monitoring cameras remains a complex task. Extracted features from the grape images need to account for gradual phenological evolution (e.g. berry size or colour changes), which can then be used to compare the behaviour between different plants. A statistical framework handling noisy datasets with complex non-linear trends within potentially incomplete temporal data (missing images) is then needed.

The main objective of this work was thus to assess the potential of the Vinelapse sensor for the temporal modelling of grape phenology. In a first part, an annotated dataset featuring daily grape images from 7 Vinelapse sensors will be presented. Then, the methodology for the extraction of three image features representing phenological evolution from May to September 2024 will be described. Finally, an exploratory study on the relevance of modelling trends as a smooth function of time to identify periods of change and model uncertainties will be developed.

Materials and methods

The Vinelapse sensor is based on the cooperation between an Arduino MKRWAN 1310 microcontroller and a Raspberry Pi microcomputer, mounted on a custom Printed Circuit Board and embedded inside a 3D printed case (Figure 1a). An external battery attached to the sensor in the field allows for roughly 4 to 5 months of battery life (Figure 1b). In 2024, 8 Vinelapse sensors were installed on an experimental plot (Château Luchey-Halde, Bordeaux, France), taking red green blue (RGB) pictures of the monitored plants each night. Sensor positions (Figure 1b) were sampled according to prior vigour zoning.
Vinelapse8 data were excluded, since most images were out of focus and slightly blurry, which is a major detriment to precise berry image processing. On the 7 remaining sensors, around 90% of the daily images were used in that study, 5% were missing or unusable images, 5% were usable but potentially difficult images (e.g. minor lighting issues, very small area grape). This means most of the image time series are incomplete and missing a few dates. Examples in Figure 2 illustrate the importance of controlled lighting, combined with night acquisitions, to reconstruct consistent grape time series.

Dataset annotation
Grape masks were extracted for each day and each sensor, resulting in a fully annotated image dataset containing only the grape areas (example in Figure 3). All annotations procedures were carried out using the Rotobrush tool from the After Effect suite, designed to propagate annotation masks to temporal neighbours and considerably speeding the annotation process.

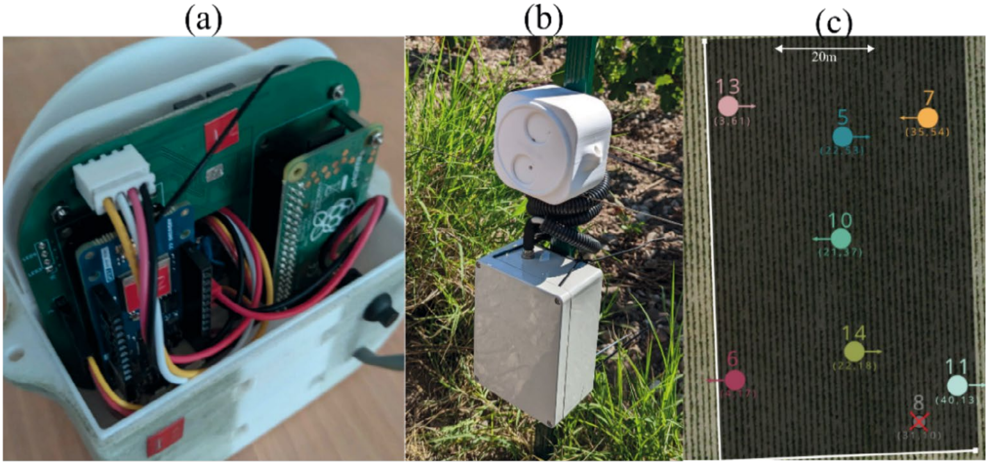

Figure 1. (a) Inside view of the sensor. (b) Photograph of the sensor installed on a post in front of a grapevine. (c) Localization of the 8 Vinelapse sensors installed in 2024 on the 'Marroniers' vineyard (WGS84 coordinates: Lat: 44.82014° N, Long: 0.63110° W). Arrows indicate the orientation of the sensors.

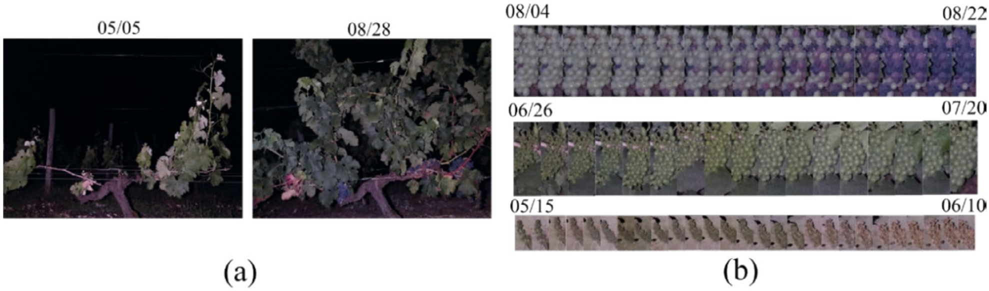

Figure 2. (a) Example of full field pictures of the same vine taken by a Vinelapse sensor. (b) Extracts of daily timelapses showcasing grape growth at different phenological stages with the same resolution, from flowering (bottom line) to veraison (top line).

Colour feature
Hue was chosen as a representative feature of colour changes throughout the season, such as the veraison shift from green hues to purple hues on red cultivars. Prior filtering was also performed on the intensity channel to exclude extremely dark or light areas. Mean hue values were then computed for each image and each day (Figure 3b).

Texture feature
Local Binary Patterns (LBPs) were chosen as the basis for simple texture description. LBPs summarize local structures of images by comparing each pixel with its neighbouring pixels (Ojala *et al.*, 1996). Important properties of the computed uniformity measure include rotation invariance. Different combinations of the (number of points in the circular neighbourhood) and R (scale) parameters were tested and applied to 48×48 patches (Figure 3a). Results, referred to as "LBP", used $P = 24$, $R = 3$ as parameters.

Berry size feature
Extracting berry radius from the grape masks is a much more challenging task than colour and texture features. As a first attempt to extract that information, part of the fruit detection approach from Keresztes *et al* (2018) was applied to Vinelapse images. In a first step, radial Hough transform was used to detect berry locations. Their radius was then computed by finding the circle maximizing the total number of points contributing to the decision, which should correspond to berry edges (Figure 3c). Only images acquired after 1 June were processed, since berries start to take form during this month.

Time series modelling
Modelling of the features time series was performed using generalized additive models (GAM) (Wood, 2017). GAM regression can be seen as a weighted sum of smooth basis functions fitting the original data in a flexible way (non-linear local trends), with a penalty parameter controlling the "wigglyness" of the functions and preventing overfitting. Using that semi-parametric regression framework, temporal features $y(t)$ can be modelled in the following way (Eq. 1):

$$y(t) = \beta_0 + \sum_{k=1}^{K} \phi_k(t)\beta_k + \varepsilon(t) \quad (1)$$

where β_0 is the intercept parameter and ϕ_k refers to penalized cubic regression splines centred at different dates (knots) and weighted by the parameters β_k. $\varepsilon(t)$ is the error term. After prior trials, $K = 12$ was chosen as the number of knots for all experiments.

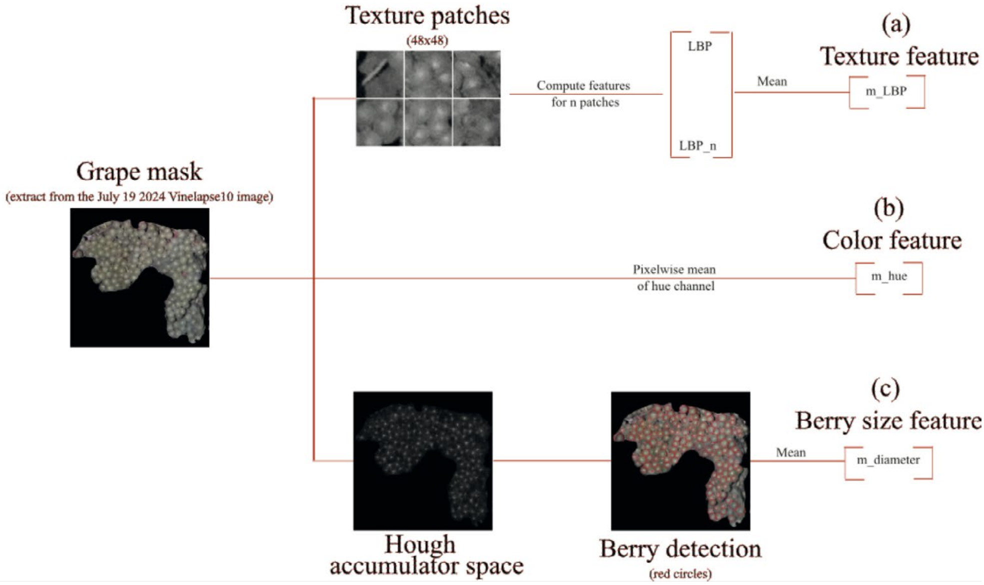

Figure 3. Extraction steps of features from a grape image. (a) Texture feature computed from 48x48 pixels patches. (b) Colour feature computed from hue histograms. (c) Mean berry size estimation using radial Hough transform.

One interesting property of GAMs is their ability to easily approximate Simultaneous Confidence Bands (SCB) from the covariance matrix of the estimated model parameters (Simpson, 2018). SCB can be seen as the smooth envelope fully containing 95% of curves drawn from the posterior distribution of the fitted model. The same process can be used on the first derivative with minor changes, meaning it is possible to compute a SCB for the estimated slope. Consequently, grape features can be evaluated on their ability to highlight significant rates of change during the season.

Results

When considering data averaged over all seven sensors, the three evaluated features (Figure 4) exhibited distinct shapes. Unsurprisingly, berry hue and radius curves featured a sharp increase during the summer, respectively at the end of July for the hue (veraison stage) and at the end of June for berry radius (growth from pea-size stage to bunch closure stage). The LBP feature is harder to interpret, featuring a peculiar V shape for all sensors, whose stationary point (global minimum) can be roughly located at the beginning of July. These changes may be explained by the texture change during flowering (coarser texture), and the reduction of the gap between berries during berry growth. As a whole, early hue and LBP measures seem more scattered. Early inflorescences are much smaller than late grapes and thus the sampled surface is lower, which also implies higher sensitivity to potential annotation errors (leaves or branches included in the grape area). Results however also show the severe shortcomings of the proposed berry radius detection algorithm. From the middle of July, berry size falls off drastically for all sensors. This is obviously not an expected behaviour, since berry size should reach a stable plateau by the end of July. These errors can be attributed to incorrect radius estimation, related to the detection of lighting halos instead of the berry edges when the berry is bigger, a phenomenon seemingly exacerbated when berries turn purple at the beginning of August (Figure 4c).

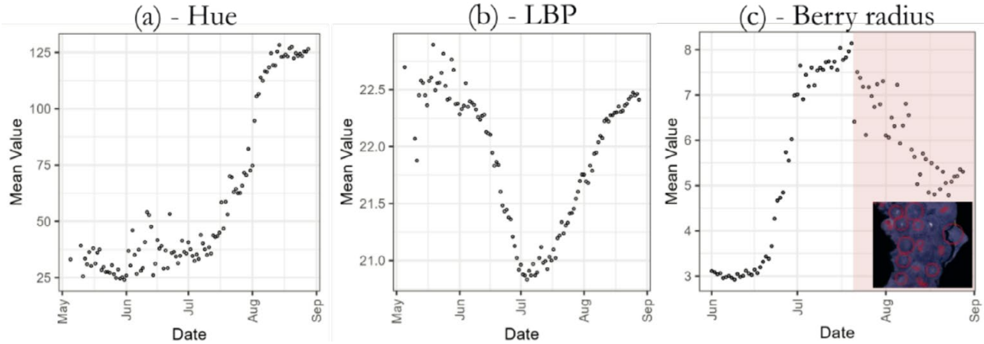

Figure 4. Mean feature values averaged over all 7 sensors. The red rectangle inside panel c indicates wrong and unexpected results in the berry radius time series, including an extract of an august grape mask detection with underestimated radiuses.

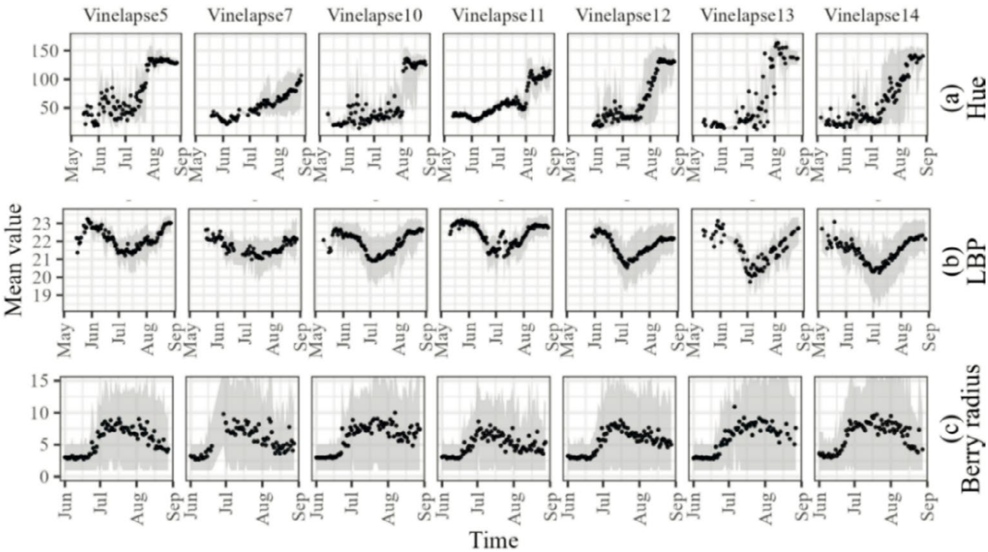

Figure 5. Feature values for each sensor. Black dots: mean time series obtained for the three features (lines) and for the 7 sensors (columns). Grey areas indicate pointwise 5% and 95% quantiles.

When considering results individually for each sensor (Figure 5), major differences were found between plants, even though global shapes remained similar. For instance, hue time series were particularly affected if stages from flowering to veraison did not occur normally due to grape hazards (e.g. millerandage, uneven ripeness), as is the case with the plant monitored by Vinelapse7. The global minimum date for all the LBP time series were similar between sensors, even though the precise dates are difficult to spot. Again, berry radius results were unsatisfactory, many false detections resulted in excessive variability (Figure 5c).

Figure 6 presents the GAM regression results on the LBP texture feature. Using relatively few functional basis ($K = 12$), a smooth representation of the underlying data was achieved (Figure 6a). While a few local trends deviate from the fitted model (e.g. Vinelapse11 during July, most likely unrelated to grape phenology), mostly narrow confidence intervals were proposed by the algorithm,

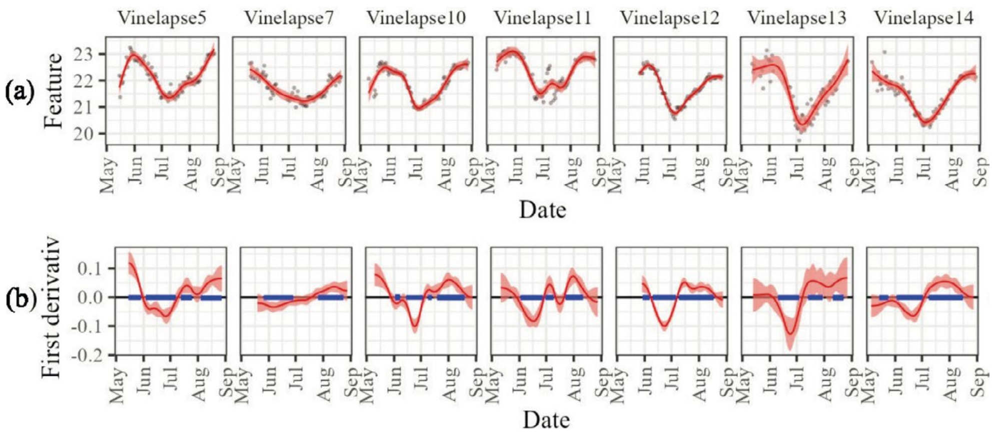

Figure 6. Example regression results for the mean LBP feature. Red line: (a) mean LBP feature GAM fit, (b) first derivative fit. Red shading: 95% SCB. Grey points: Original data. Blue horizontal lines: significant rate-of-change periods according to the SCB.

except for Vinelapse13. Based on the first derivative results (Figure 6b), it was then possible to determine which time periods have a significant rate of change according to the SCB (i.e. 95% of the curves generated from the model have a non-zero slope across the whole period). SCB approximated on the slope were wider, but certain periods (e.g. flowering to pea-size, from June to July) yielded a significant decrease of the LBP feature for all sensors. These results may be partly explained by the daily resolution of the sensor and the high amount of temporal data used to fit the model. Side experiments performed on data simulating weekly or monthly image acquisitions yielded wider SCB.

Discussion

Feature choice

Features were chosen for their simplicity in order to provide a first evaluation of the proposed grape phenology modelling framework. Additionally, temporal dependencies weren't considered during the feature extraction stage. Considering the imperfection of the features and their unknown correlation with the actual variables of interest, it is obvious the detected trends do not necessarily account for real phenomena (as seen with the berry size example) or may be wrongly interpreted. Many other image processing approaches can be developed to compute more robust features. Deep learning architectures are obvious candidates to improve the extraction step. Fine-tuned generic convolutional networks can be used to extract a set of candidate texture/colour features while specific fruit detection networks can be trained to extract berry radiuses. However, the former may lack interpretability while the latter most probably needs a dedicated annotated berry dataset covering all relevant phenological stages in order to learn the weights of the model. In this preliminary study, standard image features were thus preferred in order to identify the needs for further image processing research. Moreover, only colour images were used. The Vinelapse sensor however integrates near-infrared lighting, meaning it is possible to compute vegetation indices related to the near-infrared frequency domain.

GAMs relevance

In this study, GAMs were applied to evenly spaced time series (including missing data) with a single covariate. It is worth mentioning GAMs naturally allow the combination of different covariates and interactions. The flexibility of these modern approaches leads to interesting opportunities to combine data from different sensors sampling the field at various spatial and temporal scales. Contrary to other similar approaches such as ARIMA models, GAMs also handle unevenly sampled time series, an important property for the analysis of real field data. The parametrization and interpretability of such models can however be tricky (number of knots, basis function choice, penalty parameter estimation method, handling autocorrelated residuals if necessary), even though standardized procedures exist for simple datasets.

Conclusions

In this study, the use of a grapevine imaging sensor for the daily modelling of phenological parameters related to grapes was presented. Using simple handcrafted image features, the temporal evolution of grapes was partly described. The time series obtained highlight behaviour differences between vines monitored by the sensor. Examples making use the abilities of generalized additive models to provide uncertainties associated with the modelled trend and its first derivative were then presented. Overall, the comparison of vines based on grape image features and their rate of change is a promising way to highlight spatial phenological differences in the vineyard.

References

Ammoniaci, M., Kartsiotis, S.-P., Perria, R., & Storchi, P. (2021). State of the art of monitoring technologies and data processing for precision viticulture. Agriculture 11, 201. https://doi.org/10.3390/agriculture11030201

Darras, K.F.A., Balle, M., Xu, W., Yan, Y., Zakka, V.G., Toledo-Hernández, M., Sheng, D., Lin, W., Zhang, B., Lan, Z., Li, F., & Wanger, T.C. (2024). Eyes on nature: embedded vision cameras for terrestrial biodiversity monitoring. Methods in Ecology and Evolution, 15(12), 2262–2275. https://doi.org/10.1111/2041-210X.14436

García de Cortázar-Atauri, I., Duchêne, E., Destrac-Irvine, A., Barbeau, G., de Rességuier, L., Lacombe, T., Parker, A.K., Saurin, N., & van Leeuwen, C. (2017). Grapevine phenology in France: from past observations to future evolutions in the context of climate change. OENO ONE 51, 115–126. https://doi.org/10.20870/oeno-one.2017.51.2.1622

Keresztes, B., Abdelghafour, F., Randriamanga, D., da Costa, J.-P., & Germain, C. (2018). Real-time fruit detection using deep neural networks, In Proceedings of the 14th International Conference on Precision Agriculture. Available online at https://ispag.org/proceedings/?action=abstract&id=4956&title=Real-Time+Fruit+Detection+Using+Deep+Neural+Networks (accessed December 2024).

Mendes, J., Peres, E., Neves dos Santos, F., Silva, N., Silva, R., Sousa, J.J., Cortez, I., & Morais, R. (2022). VineInspector: the vineyard assistant. Agriculture, 12, 730. https://doi.org/10.3390/agriculture12050730

Ojala, T., Pietikäinen, M., & Harwood, D. (1996). A comparative study of texture measures with classification based on featured distributions. Pattern Recognition, 29, 51–59. https://doi.org/10.1016/0031-3203(95)00067-4

Simpson, G.L. (2018). Modelling palaeoecological time series using generalised additive models. Frontiers in Ecology and Evolution, 6, 149. https://doi.org/10.3389/fevo.2018.00149

Tardif, M., Amri, A., Keresztes, B., Deshayes, A., Martin, D., Greven, M., & Da Costa, J.-P. (2022). Two-stage automatic diagnosis of Flavescence Dorée based on proximal imaging and artificial intelligence: a multi-year and multi-variety experimental study. OENO ONE 56, 371–384. https://doi.org/10.20870/oeno-one.2022.56.3.5460

Verdugo-Vásquez, N., Acevedo-Opazo, C., Valdés-Gómez, H., Araya-Alman, M., Ingram, B., García de Cortázar-Atauri, I., & Tisseyre, B. (2016). Spatial variability of phenology in two irrigated grapevine cultivar growing under semi-arid conditions. Precision Agriculture. 17, 218–245. https://doi.org/10.1007/s11119-015-9418-5

Wood, S.N. (2017). Generalized additive models: an introduction with R, 2nd edn. Chapman and Hall/CRC, New York, NY. https://doi.org/10.1201/9781315370279